Hopping in the glass configuration space: Subaging and generalized scaling laws

Bernd Rinn,[1] Philipp Maass,[1,2] and Jean-Philippe Bouchaud[2]
[1]*Fachbereich Physik, Universität Konstanz, 78457 Konstanz, Germany*
[2]*Service de Physique de l'Etat Condensé, CEA Saclay, 91191 Gif sur Yvette Cedex, France*
(Received 11 April 2001; published 22 August 2001)

Aging dynamics in glassy systems is investigated by considering the hopping motion in a rugged energy landscape whose deep minima are characterized by an exponential density of states $\rho(E)=T_g^{-1}\exp(E/T_g)$, $-\infty<E\leqslant 0$. In particular we explore the behavior of a generic two-time correlation function $\Pi(t_w+t,t_w)$ below the glass transition temperature T_g when both the observation time t and the waiting time t_w become large. We show the occurrence of ordinary scaling behavior, $\Pi(t_w+t,t_w)\sim F_1(t/t_w^{\mu_1})$, where $\mu_1=1$ (normal aging) or $\mu_1<1$ (subaging), and the possible simultaneous occurrence of generalized scaling behavior, $t_w^{\gamma}[1-\Pi(t_w+t,t_w)]\sim F_2(t/t_w^{\mu_2})$ with $\mu_2<\mu_1$ (subaging). Which situation occurs depends on the form of the effective transition rates between the low-lying states. Employing a ''partial equilibrium concept,'' the exponents $\mu_{1,2}$ and the asymptotic form of the scaling functions are obtained both by simple scaling arguments and by analytical calculations. The predicted scaling properties compare well with Monte Carlo simulations in dimensions $d=1-1000$ and it is argued that a mean-field-type treatment of the hopping motion fails to describe the aging dynamics in any dimension. Implications for more general situations involving different forms of transition rates and the occurrence of many scaling regimes in the t-t_w plane are pointed out.

DOI: 10.1103/PhysRevB.64.104417 PACS number(s): 75.10.Nr, 05.20.−y, 02.50.−r

I. INTRODUCTION

The history of glass formation strongly affects the relaxation dynamics of glassy materials.[1,2] This dynamics is found to become slower with the ''age'' of the system, that means with the time t_w expired since the material was brought into the glassy state. Such aging phenomena have been identified in many systems and various dynamical probes. Prominent examples are shear-stress relaxations in structural glasses,[3] thermoremanent magnetizations or ac susceptibility in spin glasses.[4,5] Similar effects have been observed on the dielectric constant of dipolar glasses,[6,7] of structural glasses,[8,9] and on the structure factor of Lennard-Jones systems.[10] More recent experiments in colloidal gels[11] or other ''soft glassy materials'' have been reported,[12–16] and even electronic relaxations in Anderson insulators were found to exhibit aging effects.[17] Aging is also expected for pinned systems (pinned domain walls,[18,6] pinned vortex lines[19]), polymer melts,[20] and granular materials (see, e.g., Refs. 21 and 22).

From a theoretical point of view, several pictures have been proposed.[23] The simplest one is based on domain-coarsening ideas,[24] and is probably well suited to describe aging in, say, disordered ferromagnets where a well-defined order wants to establish across the system. However, in spin glasses and even more evidently in glasses, the idea of some long-range order that progressively invades the system is far from trivial. Mean-field models for spin glasses, which are formally equivalent to the mode coupling theory of glasses,[23] do indeed lead to aging phenomena below the glass transition. In this case, aging is of geometric origin:[25] As time grows, the system progressively exhausts the possibilities of lowering its energy, and finds itself around saddle points from which it is more and more difficult to escape. Thermal activation is irrelevant in these models. Although this picture might be justified for supercooled liquids *above* the mode-coupling temperature,[26] it certainly breaks down at lower temperature, where activated events become dominant. In this regime, one expects that a coarse-grained dynamical model of thermally activated hops between metastable states is a proper description of the dynamics. In fact, recent molecular dynamics (MD) simulations support this view.[27–29] Landscape models have been widely discussed in the past,[30,31] but their relevance for aging phenomena was recognized later.[32–35] These later developments were recently extended to treat rheological phenomena.[36]

The ''trap'' models studied up to now lead to correlation or response functions that depend on the ratio t/t_w of the observation time t to the waiting time t_w (full aging), or, for long-range correlated energy landscapes, on the ratio $\ln t/\log t_w$.[37] However, many experimental systems reveal *subaging* behavior, that is, the relevant variable is t/t_w^{μ} with $\mu<1$. Furthermore, it is possible that there exist, for given waiting time t_w, various scaling regimes in time t, which are governed by *different* relaxation times $\propto t_w^{\mu_s}$, $s=1,2,\ldots$. The occurrence of different scaling regions has recently been conjectured on the basis of analytical results for mean-field spin-glass models.[38,23] So far, however, it was not possible to illustrate intuitively these multiple time regimes by exact calculations on simpler models (see, however, Ref. 39 for an interesting discussion of these multiple time scales). In this paper we will discuss a model that allows us to demonstrate explicitly the possible occurrence of subaging behavior and multiple time scaling in a hopping model, where a point jumps among the deep (free)-energy minima E_i of a complex configuration space. Some of the results discussed in this paper already appeared in a Letter.[40]

II. HOPPING IN A RANDOM ENERGY LANDSCAPE

A. Model

Slow dynamics in glasses is often attributed to a thermally activated motion of a point (henceforth denoted as ''par-

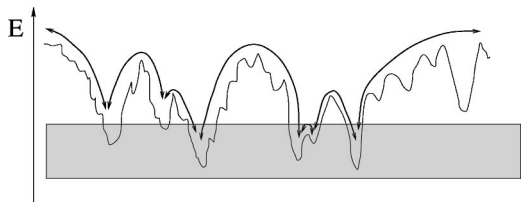

FIG. 1. Sketch of a rugged energy landscape with various metastable minima. Within a coarse-grained description, the slow dynamics of the system may be attributed to effective ''supertransitions'' between the deepest minima belonging to the shaded area.

ticle'') that jumps among metastable states in a rugged configuration space (see Fig. 1). In a coarse-grained description, only transitions between the deepest (free)-energy minima E_i will govern the dynamics at long times. According to extreme-value statistics one may expect the distribution $\psi(E)$ of these deep minima to be exponential (which is the behavior of the tail of a Gumbel distribution, see, e.g., Ref. 41). Indeed, mean-field theories of spin glasses[42] and recent results from molecular dynamics simulations[43] suggest this to be the case.

For simplicity, we consider the metastable states with lowest energies to be arranged on a hypercubic lattice in d dimensions and refer to them as ''sites.'' The lattice here resembles an average finite connectivity of the mutually accessible states. To each lattice site i is assigned a random energy E_i drawn from a distribution

$$\psi(E)=\frac{1}{T_g}\exp\left(\frac{E}{T_g}\right);\quad -\infty<E\leqslant 0. \tag{1}$$

As discussed in a moment, T_g corresponds to a ''glass transition temperature'' and we thus define

$$\theta\equiv T/T_g \tag{2}$$

as the rescaled temperature. Also, energies are specified in units of T_g. The particle can jump from one site i to any of the $2d$ nearest-neighbor sites j with a hopping rate

$$w_{i,j}=\nu\exp\left(-\frac{[\alpha E_j-(1-\alpha)E_i]}{\theta}\right), \tag{3}$$

where the ''attempt frequency'' $\nu\equiv 1$ sets our time unit, and the parameter α specifies how the energies of the initial and target site contribute to the saddle point energy being surmounted during a jump. In order for the $w_{i,j}$ to obey detailed balance, α can assume any real value, but in a sense of a weighting of the initial and target energy we restrict α to the range

$$0\leqslant\alpha<1. \tag{4}$$

Note that the case $\alpha=0$ defines a trap model, where the jump rates depend on the initial energy only, while the case $\alpha=1/2$ defines a ''force model,'' where the jump rates are determined by the energy difference between the two sites.

Due to the existence of very deep traps, the system exhibits a ''dynamical phase transition'' at the glass transition temperature $\theta=1$: in the high-temperature regime $\theta>1$ the Boltzmann distribution

$$\psi(E)e^{-E/\theta}=e^{(1-1/\theta)E} \tag{5}$$

is normalizable, while in the low temperature an equilibrium state does not exist. In this latter situation the system is exploring deeper and deeper traps as time proceeds and the overall dynamics ages.

For the trap model ($\alpha=0$) the dynamics is fully characterized by the trapping times

$$\tau\equiv\exp(E/\theta), \tag{6}$$

with distribution

$$\rho(\tau)=\theta\tau^{-1-\theta},\quad 1\leqslant\tau<\infty. \tag{7}$$

The absence of an equilibrium state for $\theta<1$ is reflected in the fact that the mean-trapping time $\langle\tau\rangle$ becomes infinite. For $\alpha>0$ it is convenient to operate with the τ defined in Eq. (6) as well, although these τ no longer have the meaning of a trapping time. The hopping rate (3) can then be written as

$$w_{i,j}=\frac{\tau_j^{\alpha}}{\tau_i^{1-\alpha}}. \tag{8}$$

At first glance the model defined here seems to be similar to the model considered earlier in Ref. 35. However, there is an important difference. In the model studied in Ref. 35 the disorder is of ''annealed'' type, i.e., the energy of each site is drawn anew from $\psi(E)$ after each jump. This can be viewed as a mean-field treatment and simplifies the problem to a great extent. As will be shown in Sec. III, in the annealed case one can map any parameters $(\theta,\alpha>0)$ to parameters $(\theta',\alpha=0)$, that means the α parameter is irrelevant. In the present model by contrast the energy disorder is ''quenched'' and such a mapping is not possible. We will show that this leads to the occurrence of much richer aging dynamics, including subaging behavior and generalized scaling forms.

B. Aging function

For studying aging properties we consider a quench from $\theta=\infty$ to $\theta<1$ at time 0, then wait for some time $t_w\gg 1$ and ask for the behavior of correlation functions followed during an observation time t after the waiting period. Since the physical observables are functions of the coordinates of the configuration space, they will essentially decorrelate after the system has undergone a single transition from one deep minimum to another one. Hence, a ''generic correlation function'' in the model is to consider the probability that the particle has not jumped between t_w and t_w+t. We denote this probability, after performing the disorder average, by $\Pi(t_w+t,t_w)$.

Let us note that $\Pi(t_w+t,t_w)$ can also be regarded[34] as the spin-spin-correlation function of the generalized Sherrington-Kirkpatrick model with p-spin interactions in the limit $p\to\infty$, which maps onto the random-energy

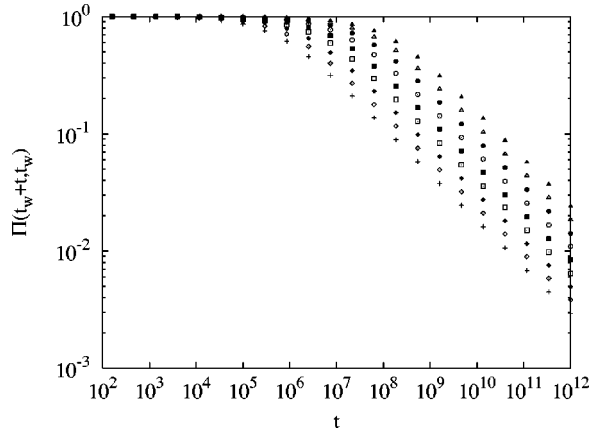

FIG. 2. Aging function $\Pi(t+t_w,t_w)$ for $(d,\theta,\alpha)=(10,1/4,3/8)$ and different waiting times t_w. The symbols refer to waiting times $t_w=2\times10^8(+)$, 5×10^8 ($\diamond$), 2×10^9 ($\blacklozenge$), 5×10^9 ($\square$), 1×10^{10} ($\blacksquare$), $4\times10^{10}(\bigcirc)$, 1×10^{11} ($\bullet$), 3×10^{11} ($\triangle$), and 1×10^{12} ($\blacktriangle$), respectively.

model.[44] It can also be viewed as an incoherent intermediate scattering function at large wave numbers in diffusion processes.[35]

A typical result for $\Pi(t+t_w,t_w)$ from continuous-time Monte Carlo simulations is shown in Fig. 2 for parameters $(d,\theta,\alpha)=(10,1/4,3/8)$ and different t_w (for details regarding the simulation see Appendix A). Indeed, we can identify a pronounced aging phenomenon: The decay of $\Pi(t_w+t,t_w)$ with time t becomes slower and slower with increasing waiting time t_w. The linear behavior of the curves at long times in the double-logarithmic plot indicates a common asymptotic power-law decay, and suggests that the various curves may be collapsed onto a common master after rescaling the observation time t by a proper function of the waiting time t_w. The understanding of such scaling properties of $\Pi(t+t_w,t_w)$ when both t and t_w become large $(t,t_w\gg1)$ will be the central issue in the following.

III. ANNEALED SITUATION

In the annealed case the model corresponds to a continuous-time random walk (CTRW) irrespective of the value of α, since all times τ_j are drawn anew after each transition. The whole process can be characterized by a distribution $\rho_{\rm eff}(\tau_{\rm eff})$ of effective trapping times $\tau_{\rm eff}$ (residence times between two transitions).

In order to calculate $\rho_{\rm eff}(\tau_{\rm eff})$, let us consider the particle to be at site $i=0$. Then

$$\tau_{\rm eff}=\frac{1}{\sum_{j=1}^{2d} w_{0,j}}=\frac{\tau_0^{1-\alpha}}{\sum_{j=1}^{2d}\tau_j^{\alpha}}, \tag{9}$$

and the distribution is given by

$$\begin{aligned}\rho_{\rm eff}(\tau_{\rm eff})&=\left[\prod_{i=0}^{2d}\int_1^\infty d\tau_i\rho(\tau_i)\right]\delta\left(\tau_{\rm eff}-\frac{\tau_0^{1-\alpha}}{\sum_{j=1}^{2d}\tau_j^{\alpha}}\right)\\&=\left[\prod_{i=0}^{2d}\int_1^\infty d\tau_i\rho(\tau_i)\right]\frac{\tau_{\rm eff}^{\alpha/(1-\alpha)}}{1-\alpha}\left[\sum_{j=1}^{2d}\tau_j^{\alpha}\right]^{1/(1-\alpha)}\\&\quad\times\delta\left(\tau_0-\tau_{\rm eff}^{1/(1-\alpha)}\left[\sum_{j=1}^{2d}\tau_j^{\alpha}\right]^{1/(1-\alpha)}\right).\end{aligned} \tag{10}$$

The δ function contributes if $\tau_{\rm eff}\Sigma_{j=1}^{2d}\tau_j^{\alpha}\geqslant1$, i.e., there is no restriction for $\tau_{\rm eff}\geqslant1/2d$. Hence, for $\tau_{\rm eff}\geqslant1/2d$:

$$\rho_{\rm eff}(\tau_{\rm eff})=C_{\rm eff}\theta'\tau_{\rm eff}^{-1-\theta'},\quad \theta'\equiv\frac{\theta}{(1-\alpha)}, \tag{11}$$

where $C_{\rm eff}=\langle[\Sigma_{j=1}^{2d}\tau_j^{\alpha}]^{-\theta'}\rangle$, and $\langle\ldots\rangle$ denotes an average over $2d$ uncorrelated random numbers τ_j distributed according to Eq. (7). The CTRW theory applies with a rescaled temperature θ', and the aging properties of this model have been worked out in Ref. 35.

Note in particular that for $\theta'>1$ no aging occurs, even if the distribution (5) is not normalizable for $\theta<1$. This, however, is nothing to worry about, since in the annealed model the energies change after each hop and the distribution (5) does not correspond to an equilibrium distribution. The dynamical phase transition in the annealed model is defined by the diverging mean waiting time of the distribution $\rho_{\rm eff}(\tau_{\rm eff})$ that occurs for $\theta'<1$. The absence of aging for $0<1-\theta<\alpha$, that is when $\theta'>1$ but $0<\theta<1$, points to the fact that the annealed model may not provide a valid mean-field description of the quenched model in any dimension d.

In Fig. 3 the aging function $\Pi(t_w+t,t_w)$ is shown for the annealed model as resulting from simulations for two different parameters sets, $(d,\theta,\alpha)=(10,1/3,0)$ and $(d,\theta,\alpha)=(10,1/4,1/4)$ that both refer to the same $\theta'=1/3$. As expected, the aging functions for the two parameter sets are indistinguishable. Moreover, as predicted in Ref. 34, $\Pi(t_w+t,t_w)$ scales with t/t_w, $\Pi(t_w+t,t_w)=F(t/t_w)$, where $F(u)\sim1-u^{1-x}$ for $u\ll1$ [see Fig. 3(b)] and $F(u)\sim u^{-x}$ [see Fig. 3(a)]. We will see in the following that this simple behavior does not hold true any longer in the quenched case. Nevertheless, since $\tau_{\rm eff}$ is the inverse hopping rate on a site, the formulas (9) and (11) will still be useful in the following.

IV. PARTIAL EQUILIBRIUM CONCEPT (PEC)

Although full equilibrium cannot be reached in a system of infinite size, there should be some equilibration on a local scale that corresponds to the region of configuration space being explored by the system after the quench. This is the idea of the PEC.

In the present model we can translate this idea into a precise though approximate procedure for describing the aging process. After the waiting time t_w, the particle has visited $S=S(t_w)$ distinct sites and we will assume that on these sites the system has equilibrated. Accordingly, the probabil-

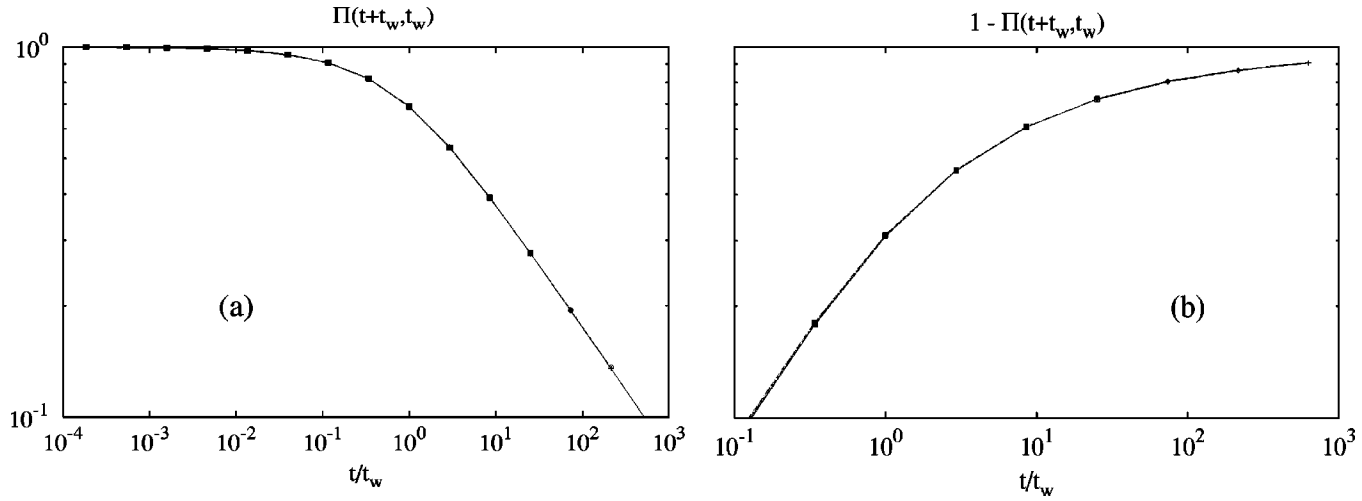

FIG. 3. Aging functions (a) $\Pi(t+t_w,t_w)$ and its complement (b) $1-\Pi(t+t_w,t_w)$ from simulations of the annealed model with parameters $(d,\theta,\alpha)=(10,1/3,0)$ (lines) and $(d,\theta,\alpha)=(10,1/4,1/4)$ (points). The waiting times range from 10^9 to 10^{12}. The scaling is so good that the various curves cannot be distinguished on the scale of the line thickness. The tick labels of the ordinate of part (a) refer also to part (b).

ity p_j to find the particle on the site j of the set of visited sites is

$$p_j(S)=\frac{e^{-E_j/\theta}}{\sum_{k=1}^{S} e^{-E_k/\theta}}=\frac{\tau_j}{\sum_{k=1}^{S}\tau_k}. \tag{12}$$

The probability for the particle to remain on site j for a time t is $\exp(-t\Sigma_{n_j}w_{j,n_j})=\exp(-t\tau_j^{\alpha-1}\Sigma_{n_j}\tau_{n_j}^{\alpha})$, where the sum over n_j runs over all nearest-neighbor sites of j. Since the distinct visited sites form a Brownian path in the lattice, which, on a local scale, has a one-dimensional topology, we will consider exactly two of the n_j sites to belong to the path. The remaining $n-2$ sites are considered to be never visited until t_w. It will turn out (see Sec. VII) that this assumption is not very important and that the aging properties would be mainly the same if the Brownian path had a compact structure (except for the asymptotics discussed in Sec. VII F). According to the PEC, the aging function $\Pi(t_w+t,t_w)$ is now approximated by taking the average of $\exp(-t\tau_j^{\alpha-1}\Sigma_{n_j}\tau_{n_j}^{\alpha})$ over all visited sites j with the weights p_j,

$$\tilde{\Pi}(t_w+t,t_w)\equiv\left\langle\frac{\sum_{j=1}^{S(t_w)}\tau_j\exp\left(-t\tau_j^{\alpha-1}\sum_{n_j}\tau_{n_j}^{\alpha}\right)}{\sum_{k=1}^{S(t_w)}\tau_k}\right\rangle. \tag{13}$$

Here $\langle\ldots\rangle$ denotes an average over $(2d-1)S(t_w)$ uncorrelated random numbers τ_j that are distributed according to Eq. (7). We will see that $\tilde{\Pi}(t_w+t,t_w)$ and $\Pi(t_w+t,t_w)$ exhibit the same scaling properties, which in view of the generic character of $\Pi(t_w+t,t_w)$ (cf. Sec. II B) are of primary interest for us here. In quantitative terms both functions turn out to be different. Since $\tilde{\Pi}(t_w+t,t_w)$ depends on t_w only through $S=S(t_w)$, we will, in the following, also denote this function by $\tilde{\Pi}(t,S)$.

As shown in Appendix B, the number of distinct visited sites $S(t_w)$ grows with increasing waiting time t_w as

$$S(t_w)\sim t_w^{\gamma}, \tag{14a}$$

where

$$\gamma=\begin{cases}\dfrac{d\,\theta}{d+(2-d)\,\theta} & \text{for} \quad d<2\\ \theta & \text{for} \quad d>2.\end{cases} \tag{14b}$$

In $d=2$ there are logarithmic corrections, $S(t_w)\sim[t_w/\ln t_w]^{\theta}$.

V. SIMPLE SCALING ARGUMENTS

In this section we present simple arguments, why and how $\tilde{\Pi}(t_w+t,t_w)$ is expected to scale. In particular we propose the presence of two characteristic relaxation times $t_i(t_w)$, $i=1,2$, that grow as power laws with t_w

$$t_i(t_w)\sim t_w^{\mu_i}, \tag{15}$$

where μ_i are exponents depending on θ and α.

The first characteristic relaxation time $t_1(t_w)$ can be obtained as follows. After the waiting time t_w, the particle has visited $S=S(t_w)$ distinct sites and the occupation probability of these sites is dominated by the one for the site with lowest energy $E_{\min}$ (in the glassy phase $\theta<1$ the extreme values are dominant). The typical value of $E_{\min}$ can be estimated from $S\int_{-\infty}^{E_{\min}}\psi(E)=S\exp(E_{\min})\simeq 1$, i.e.,

$$E_{\min}(t_w)\sim-\ln S(t_w)\sim-\gamma\ln(t_w), \tag{16}$$

or, in terms of the variable $\tau_{\max}$ corresponding to $E_{\min}$,

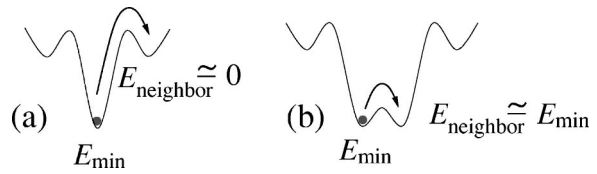

FIG. 4. Jumps out of a valley with energy $E_{\min}$ after time t_w: (a) a situation corresponding to the typical situation, where the energies of the neighboring valleys have values close to zero; (b) a rare event where at least one of the neighboring valleys has an energy of order $E_{\min}$.

$$\tau_{\max}(t_w) = \exp(-E_{\min}/\theta) \sim S(t_w)^{1/\theta} \sim t_w^{\gamma/\theta}. \tag{17}$$

Being at the site with energy $E_{\min}$, the particle typically encounters a situation as drawn in Fig. 4(a): All neighboring sites have energies close to zero and the characteristic escape time t_1 from the site with energy $E_{\min}$ is the inverse hopping rate given in Eq. (9), $t_1(t_w) \sim \tau_{\max}^{1-\alpha} \sim S^{(1-\alpha)/\theta} \sim t_w^{\gamma(1-\alpha)/\theta}$, i.e.,

$$\mu_1 = \frac{\gamma(1-\alpha)}{\theta}. \tag{18}$$

Hence, for both t and t_w becoming large ($t, t_w \gg 1$) and $\Lambda_1 = t/t_w^{\mu_1}$ being fixed we expect $\tilde{\Pi}(t,S)$ to become a function of Λ_1 only

$$\tilde{\Pi}(t,S) \sim F_1(\Lambda_1), \quad \Lambda_1 = t/t_w^{\mu_1}. \tag{19}$$

The second relaxation time $t_2(t_w)$ is associated with rare events depicted in Fig. 4(b), which turn out to be important at small times. The deepest state on an interval of length S has a typical value determined by the fact that it should occur with a probability $1/S$. To obtain the scaling of the second deepest state with S we note that for a distribution exhibiting no peculiar long-time tails, the gap between the deepest and second-deepest state remains finite when $S \to \infty$. Accordingly, with probability of order $1/S \sim \tau_{\max}^{-\theta}$ one of the neighboring sites can also have an energy comparable to $E_{\min}$. In this case the hopping rate specified in Eq. (8) yields $t_2 \sim \tau_{\max}^{1-\alpha}/\tau_{\max}^{\alpha} \sim S^{(1-2\alpha)/\theta}$, i.e.,

$$\mu_2 = \frac{\gamma(1-2\alpha)}{\theta}. \tag{20}$$

Clearly this is a relevant time growing with t_w only for $\alpha < 1/2$. Moreover, there is a further condition on the relevance of t_2. To see this, we may consider the formal short-time expansion of $\tilde{\Pi}(t,S)$ from Eq. (13). Using the fact that a sum over random τ's raised to some power with an exponent larger than θ scales as the maximal term appearing in the sum (Lévy statistics), we can estimate

$$\tilde{\Pi}(t,S) = \left\langle \sum_{m=0}^{\infty} \frac{(-t)^m}{m!} \sum_{j=1}^{S} p_j \tau_j^{-(1-\alpha)m} \left(\sum_{n_j} \tau_{n_j}^{\alpha} \right)^m \right\rangle$$
$$\simeq 1 + \sum_{m=1}^{\infty} \frac{(-t)^m}{m!\, \tau_{\max}^{(1-\alpha)m}} [1 + \tau_{\max}^{-\theta} \tau_{\max}^{\alpha m}]. \tag{21}$$

Here the first term in the rectangular brackets corresponds to the typical situation, while the second term corresponds to the rare events and is weighted by a factor $\tau_{\max}^{-\theta}$ (we have neglected constant prefactors). Comparing these two terms, we see that, if $\theta < \alpha$, the latter term dominates for *all* m. In this case we thus expect the scaling behavior of the form

$$S[1 - \tilde{\Pi}(t,S)] \sim F_2(\Lambda_2), \quad \Lambda_2 = t/t_2(t_w) \tag{22}$$

for times $t, t_w \gg 1$ and $\theta < \alpha < 1/2$.

For $\alpha < \theta$ to the contrary, the first term in the rectangular brackets dominates for small $1 \leqslant m \leqslant \theta/\alpha$, and $t_2(t_w)$ is not significant [note that $t_2(t_w)$ is smaller than $t_1(t_w)$]. The fact that Eq. (21) is not a regular expansion in the scaling variable $t/t_1(t_w) = t/\tau_{\max}^{1-\alpha}$ (for $\alpha > 0$) indicates that $F_1(\Lambda_1)$ does not have an analytical behavior for small Λ_1. On the other hand, the formal short-time expansion suggests a regular behavior $F_2(\Lambda_2) \sim \Lambda_2$. An exact treatment of the PEC formula (13) presented in Sec. VII, however, shows that this should be true only in $d=1$. The small Λ_2 regime is in fact a subtle one since it is very sensitive to rare events and the connectivity properties of the Brownian path.

We can furthermore deduce the asymptotic form of $F_1(\Lambda_1)$ for $\Lambda_1 \to \infty$ and $\Lambda_1 \to 0$ by simple arguments as will be shown next. The behavior of $F_2(\Lambda_2)$ for large Λ_2 then follows from the fact that the large Λ_2 behavior of Eq. (22) should match the small Λ_1 behavior of Eq. (19), i.e. $1 - S^{-1} F_2(t/t_w^{\mu_2}) \simeq F_1(t/t_w^{\mu_1})$ for $1 \ll t_w^{\mu_2} \ll t \ll t_w^{\mu_1}$.

A. Limit $\Lambda_1 \to \infty$

The particle leaves the site reached after t_w typically in a time $t_w^{\mu_1}$. In order to explore the behavior for large $\Lambda_1 = t/t_w^{\mu_1} \gg 1$ we may assume $t \gg t_w \gg 1$ and ask, which events give rise to a nonvanishing $\tilde{\Pi}(t,S)$. These are *rare* events, where an unusual large inverse hopping rate $\tau_{\text{eff}} \geqslant t + t_w \simeq t$ has been encountered before the time t_w has passed, or, said differently, before the particle has visited $S(t_w)$ distinct sites. The probability that τ_{eff} on one site is smaller than t is $\mathcal{P}(t) = \int_0^t d\tau_{\text{eff}} \rho_{\text{eff}}(\tau_{\text{eff}}) \sim 1 - t^{-\theta/(1-\alpha)}$ and the probability that at least for one of $S = S(t_w)$ sites τ_{eff} is larger than t is $1 - \mathcal{P}^S$. Hence,

$$\tilde{\Pi}(t,S) \sim 1 - \mathcal{P}^S = 1 - (1-\mathcal{Q})^S \sim S(t_w)\mathcal{Q}(t), \tag{23}$$

where $\mathcal{Q}(t) = 1 - \mathcal{P}(t) \sim t^{-\theta/(1-\alpha)}$. Inserting $S(t_w)$ from Eq. (14a) we thus obtain

$$F_1(\Lambda_1) \sim \Lambda_1^{-\delta}, \quad \delta \equiv \frac{\theta}{1-\alpha}. \tag{24}$$

B. Limit $\Lambda_1 \to 0$

In the limit $\Lambda_1 \to 0$ corresponding to $1 \ll t \ll t_w^{\mu_1}$, the *typical* situations govern the decay of $\tilde{\Pi}(t_w + t, t_w)$. In these typical situations, energies $E \ll E_{\min}(t_w)$ or Boltzmann factors $\tau \gg \tau_{\max}(t_w)$ do not matter. Let us then consider a jump of the particle from a site with energy E_1 [Boltzmann factor $\tau_1 = \exp(-E_1/\theta)$] to a neighboring site with energy E_2

[Boltzmann factor $\tau_2=\exp(-E_2/\theta)$], where $0\leqslant E_1,E_2\leqslant E_{\min}$. On average such a jump occurs at a time $\tau_2^{\alpha}/\tau_1^{1-\alpha}$. The probability for the particle to be at a site with energy in an interval (E_1,E_1+dE_1) is $\psi(E_1)\exp(-E_1/\theta)dE_1 \propto \tau_1^{-1-\theta}\tau_1 d\tau_1$ (equilibrated initial site) and the probability for the energy of a neighboring site to be in an interval (E_2,E_2+dE_2) is $\psi(E_2)dE_2\propto\tau_2^{-1-\theta}d\tau_2$ (random target site). Hence the probability $\psi(t)dt$ for the particle to leave the site reached after t_w in a time interval $(t,t+dt)$ can be estimated by

$$\psi(t,\tau_{\max})\propto\int_1^{\tau_{\max}}d\tau_1\tau_1^{-\theta}\int_1^{\tau_{\max}}d\tau_2\tau_2^{-1-\theta}\delta\left(t-\frac{\tau_1^{1-\alpha}}{\tau_2^{\alpha}}\right) =:\phi(t,\tau_{\max}). \tag{25}$$

Normalizing $\psi(t)$ on its support $\tau_{\max}^{-\alpha}\leqslant t\leqslant\tau_{\max}^{1-\alpha}$ we obtain

$$\psi(t,\tau_{\max})=\frac{\phi(t,\tau_{\max})}{\int_{\tau_{\max}^{-\alpha}}^{\tau_{\max}^{1-\alpha}}dt'\ \phi(t',\tau_{\max})}. \tag{26}$$

Since $1-\tilde{\Pi}(t_w+t,t_w)$ is the probability of the particle to leave the site reached after t_w within the time interval $[0,t)$, we expect

$$1-\tilde{\Pi}(t_w+t,t_w)\sim\int_0^t dt'\ \psi(t',\tau_{\max}(t_w)) \tag{27}$$

for $t,t_w\gg 1$ and $t/t_w^{\mu_1}\ll 1$. Performing the integrals in Eq. (25) gives

$$\phi(t,\tau_{\max})=\frac{1-\alpha}{\alpha-\theta}t^{(\alpha-\theta)/(1-\alpha)}\left[\left(\frac{t}{\tau_{\max}^{1-\alpha}}\right)^{-(\alpha-\theta)/[(1-\alpha)\alpha]}-1\right]. \tag{28}$$

Since $t/\tau_{\max}^{1-\alpha}\sim\Lambda_1$, we have, in the limit $\Lambda_1\to 0$, to distinguish between $\alpha>\theta$ and $\alpha<\theta$, yielding

$$\phi(t,\tau_{\max})\sim\begin{cases}\dfrac{1-\alpha}{\alpha-\theta}t^{-(1+\theta)/\alpha}\tau_{\max}^{(1-\theta)/\alpha}, & \alpha>\theta\\ \dfrac{1-\alpha}{\theta-\alpha}t^{-1+(1-\theta)/(1-\alpha)}, & \alpha<\theta.\end{cases} \tag{29}$$

Inserting this into Eqs. (26) and (27) and using (17) then gives

$$1-F_1(\Lambda_1)\sim\Lambda_1^{\varepsilon},\quad \Lambda_1\to 0. \tag{30a}$$

with

$$\varepsilon=\begin{cases}\varepsilon_>\equiv\dfrac{\theta}{\alpha}, & \alpha>\theta\\ \varepsilon_<\equiv\dfrac{1-\theta}{1-\alpha}, & \alpha<\theta.\end{cases} \tag{30b}$$

As discussed above, by matching this small Λ_1 behavior of $F_1(\Lambda_1)$ to the large Λ_2 behavior of $F_2(\Lambda_2)$ we furthermore obtain for $\alpha>\theta$

$$F_2(\Lambda_2)\sim\Lambda_2^{\theta/\alpha},\quad \Lambda_2\to\infty. \tag{31}$$

VI. TEST OF THE PEC

A. Scaling properties

In order to test the PEC, we performed simulations of the model in $d=1$, 10, 100, and 1000 by means of a continuous-time Monte Carlo algorithm (see Appendix A for details of the simulation procedure). Averages were taken over 10^5 (for $d=1,10,100$) and 10^4 (for $d=1000$) energy landscapes.

Figures 5(a) and 5(b) show, respectively, $\Pi(t+t_w,t_w)$ and $1-\Pi(t+t_w,t_w)$ as a function of the scaled variable $\Lambda_1=t/t_w^{\mu_1}$ [cf. Eqs. (18) and (19)] for $(\theta,\alpha)=(1/4,3/8)$, i.e., a case where $\alpha>\theta$. As expected from the PEC and the scaling arguments outlined in the previous section the data collapse onto master curves $F_1(\Lambda_1)$ for all dimensions d. In particular we find $F_1(\Lambda_1)\sim\Lambda_1^{\epsilon_<}$ for $\Lambda_1\to 0$ and $F_1(\Lambda_1)\sim\Lambda_1^{-\delta}$ in agreement with Eqs. (30a,b) and (24), respectively.

Correspondingly scaled data for $(\theta,\alpha)=(1/3,1/4)$, i.e., a case where $\alpha<\theta$, are shown in Fig. 6. Again there is a good data collapse and the scaling functions $F_1(\Lambda_1)$ have the expected asymptotic behavior for small and large Λ_1. In particular we now find $F_1(\Lambda_1)\sim\Lambda_1^{\epsilon_>}$ with $\epsilon_>$ from Eq. (30a).

Moreover, for $\alpha>\theta$, PEC and the scaling arguments predict the presence of a second time scale $t_2=t_w^{\mu_2}$ [cf. Eq. (20)] and an associated generalized scaling $t_w^{\gamma}[1-\Pi(t+t_w,t_w)]\sim F_2(t/t_w^{\mu_2})$ [cf. Eqs. (22) and (14a)]. The occurrence of this generalized scaling is verified in Fig. 7 for $d=1$, 10, and 100. The master curves scale $F_2(\Lambda_2)\sim\Lambda_2^{\theta/\alpha}$ for $\Lambda_2\to\infty$ as predicted by Eq. (31). A critical reader may note that the simulated data do not collapse at large Λ_2, the deviations from scaling setting in at larger Λ_2 for larger t_w. The reason for this is that the limits $t_w\to\infty$ and $\Lambda_2=t/t_w^{\mu_2}\to\infty$ must not be commuted. One first has to take the limit $t_w\to\infty$ to obtain the scaling function $F_2(\Lambda_2)$ and then has to consider the asymptotic behavior for large Λ_2.

The behavior for $\Lambda_2\to 0$ is not so clear. For $d>1$, the exact treatment of the PEC formula (13) yields $F_2(\Lambda_2)\sim\Lambda_2^{\theta/\alpha}$ also (with a smaller prefactor in the scaling law), while for $d=1$, $F_2(\Lambda_2)\sim\Lambda_2$ seems to be correct. In fact, for $d=1$ the data in Fig. 7 are in fair agreement with a linear behavior. For $d=10,100$ the data also show some linear dependence for intermediate Λ_2 values (see the dashed lines in Fig. 7), and in fact, such intermediate regime is predicted to occur based on the PEC formula (although it should be less pronounced, see the discussion in Sec. VII F). For very small Λ_2, however, we expect $F_2(\Lambda_2)\sim\Lambda_2^{\theta/\alpha}$, although this asymptotic regime can not be identified in Fig. 7. At best we can say that there is a change in curvature at very small Λ_2. The true asymptotics, however, could not be obtained within reasonable CPU time.

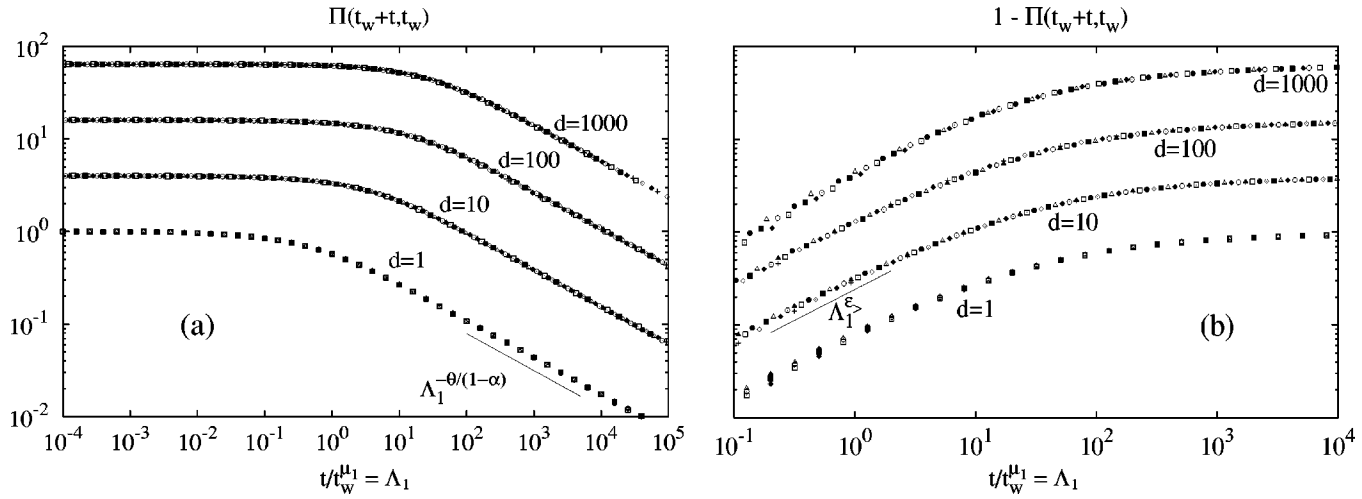

FIG. 5. First scaling function for a parameter set with $\alpha > \theta$: (a) $\Pi(t_w+t,t_w)$ and (b) $1-\Pi(t_w+t,t_w)$ as a function of $t/t_w^{\mu_1}=\Lambda_1$ for parameters $(\theta,\alpha)=(1/4,3/8)$ and different dimensions d. The straight lines indicate the asymptotic behavior according to Eqs. (24) and (30). In order to make the graphs distinguishable, $\Pi(t_w+t,t_w)$ and $1-\Pi(t_w+t,t_w)$ have been multiplied by factors 4, 16, and 64 for $d=10$, 100, and 1000, respectively. In plot (b) also $t/t_w^{\mu_1}$ has been multiplied by factors 32, 4, 1, and 0.5 for $d=1$, 10, 100, and 1000, respectively. For $d=10$ and $d=100$ the symbols refer to the same waiting times as in Fig. 2. For $d=1$ the symbols refer to $t_w=6\times10^6$ (+), 2×10^7 (◇), 4×10^7 (♦), 1×10^8 (□), 3×10^8 (■), 6×10^8 (○), 2×10^9 (●), 4×10^9 (△), and 1×10^{10} (▲). For $d=1000$ the symbols refer to $t_w=6\times10^6$ (♦), 1×10^7 (□), 3×10^7 (■), 8×10^7 (○), 2×10^8 (●), and 4×10^8 (△). The tick labels of the ordinate of part (a) refer also to part (b).

Accounting for the existence of two different time scales is very important to properly rescale the numerical results. Had one assumed a single time scale t_w^{μ}, one would have obtained an approximate data collapse with an effective value of μ intermediate between μ_1 and μ_2. This remark might be of importance for analyzing experimental data: the assumption of a single time scale could lead to a systematic underestimation of the true, asymptotic value of μ (see the discussion in Ref. 45).

B. Full comparison with simulations

While the predictions of PEC regarding the scaling properties and the asymptotic behavior of the scaling functions are fulfilled, $\Pi(t+t_w,t_w)$ and its PEC equivalent $\tilde{\Pi}(t+t_w,t_w)$ are different in quantitative terms. To see this, we have computed $\tilde{\Pi}(t+t_w,t_w)$ numerically according to Eq. (13) and compared it with $\Pi(t+t_w,t_w)$ obtained from the Monte Carlo simulations. As shown in Fig. 8 the scaling functions associated with $\Pi(t+t_w,t_w)$ and $\tilde{\Pi}(t+t_w,t_w)$ dif-

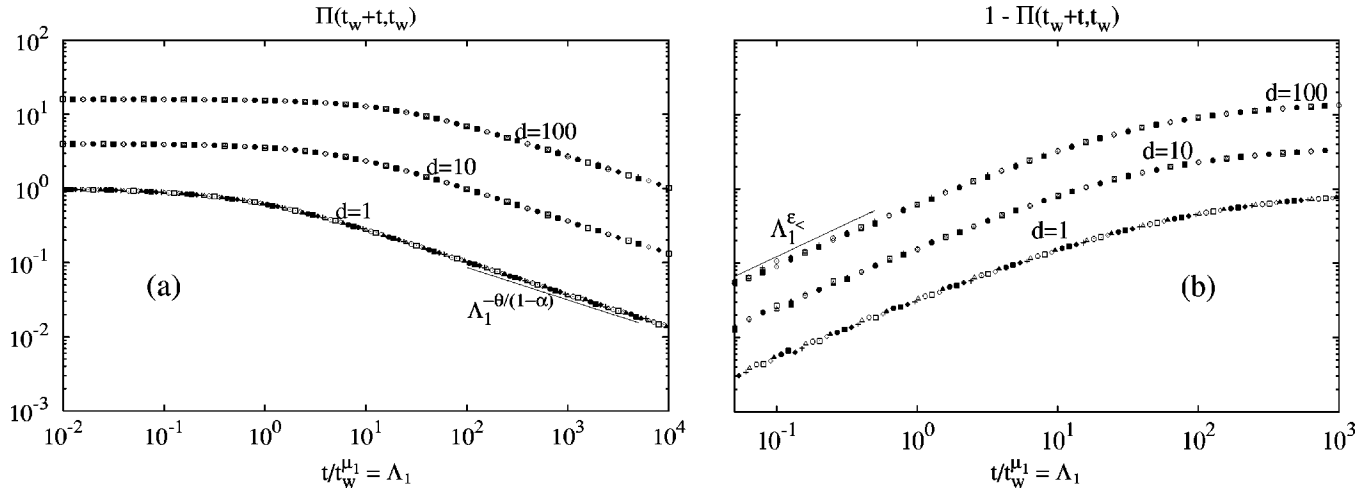

FIG. 6. First scaling function for a parameter set with $\alpha < \theta$: (a) $\Pi(t_w+t,t_w)$ and (b) $1-\Pi(t_w+t,t_w)$ as a function of $t/t_w^{\mu_1}=\Lambda_1$ for $(\theta,\alpha)=(1/3,1/4)$ and different dimensions d. The straight lines indicate the asymptotic behavior according to Eqs. (24) and (30). In order to make the graphs distinguishable $\Pi(t_w+t,t_w)$ and $1-\Pi(t_w+t,t_w)$ have been multiplied by factors 4 and 16 for $d=10$ and 100, respectively. In plot (b) also $t/t_w^{\mu_1}$ has been multiplied by factors 32 and 4 for $d=1$ and 10, respectively. The symbols refer to the same waiting time as for $d=1$ in Fig. 5. The tick labels of the ordinate of part (a) refer also to part (b).

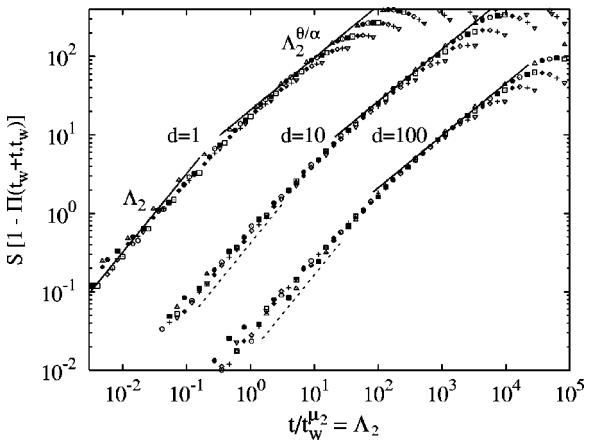

FIG. 7. Scaling function $F_2(\Lambda_2)$ for the same parameter set as in Fig. 6: $S[1-\Pi(t_w+t,t_w)]$ as a function of $t/t_w^{\mu_2}=\Lambda_2$ for $(\theta,\alpha)=(1/4,3/8)$ and $d=1,10,100$. The straight lines for large Λ_2 indicate the asymptotic behavior according to Eq. (31), while the solid ($d=1$) and dashed lines ($d=10,100$) for small Λ_2 correspond to a linear behavior (see text). The symbols refer to the same waiting times as in Fig. 5, with the additional waiting time $t_w=3\times10^6$. In order to make the graphs distinguishable, $S[1-\Pi(t_w+t,t_w)]$ has been multiplied by factors 10 and 5 for $d=1$ and 10, respectively.

fer by a factor in the scaling variable and the precise form in a transient region between the asymptotic regimes for small and large arguments.

In summary we can conclude that all predictions of the PEC concerning the scaling properties can be corroborated by the simulations. The PEC thus turns out to be a powerful tool to uncover the mechanisms of aging in quenched random energy landscapes.

VII. EXACT EVALUATION OF THE PARTIAL EQUILIBRIUM FORMULA

In this part we show how the scaling arguments presented in Sec. V can be validated by an exact evaluation of the PEC formula (13) in the limit of large S (large t_w). The reader who is not interested in these more mathematical derivations, may skip this section and proceed with the Summary in Sec. VIII.

When we replace the denominator of Eq. (13) by $\int_0^\infty d\lambda\, \exp(-\lambda\Sigma_{k=1}^S \tau_k)$ and notice that all but three random τ_k are uncorrelated with the τ_j, τ_{n_j} appearing in the numerator of Eq. (13), we find

$$\tilde{\Pi}(t,S)=S\int_0^\infty d\lambda \langle e^{-\lambda\tau}\rangle^{S-3} g(t;\lambda), \tag{32}$$

where $g(t;\lambda)$ is defined by

$$\begin{aligned} g(t;\lambda) &\equiv \left\langle \tau \exp\left[-t\tau^{\alpha-1}\sum_{j=1}^{2d}\tau_j^\alpha - \lambda(\tau+\tau_1+\tau_2)\right]\right\rangle \\ &= \int_1^\infty \frac{\theta\, d\tau}{\tau^\theta} e^{-\lambda\tau}\int_1^\infty \frac{\theta\, d\tau_1}{\tau_1^{1+\theta}} e^{-\lambda\tau_1}\int_1^\infty \frac{\theta\, d\tau_2}{\tau_2^{1+\theta}} e^{-\lambda\tau_2} \\ &\quad \times \exp\left(-t\frac{\tau_1^\alpha+\tau_2^\alpha}{\tau^{1-\alpha}}\right)\left[f\left(\frac{t}{\tau^{1-\alpha}}\right)\right]^{2(d-1)} \end{aligned} \tag{33}$$

and

$$f(z)\equiv \int_1^\infty \frac{\theta\, d\tau}{\tau^{1+\theta}} e^{-z\tau^\alpha} = \frac{\theta}{\alpha} z^{\theta/\alpha}\Gamma\left(-\frac{\theta}{\alpha}, z\right). \tag{34a}$$

Here $\Gamma(a,z)=\int_z^\infty dt\, e^{-t}t^{a-1}$ denotes the incomplete Gamma function. Note that $0\leqslant f(z)\leqslant 1$ and that for $z\to 0$

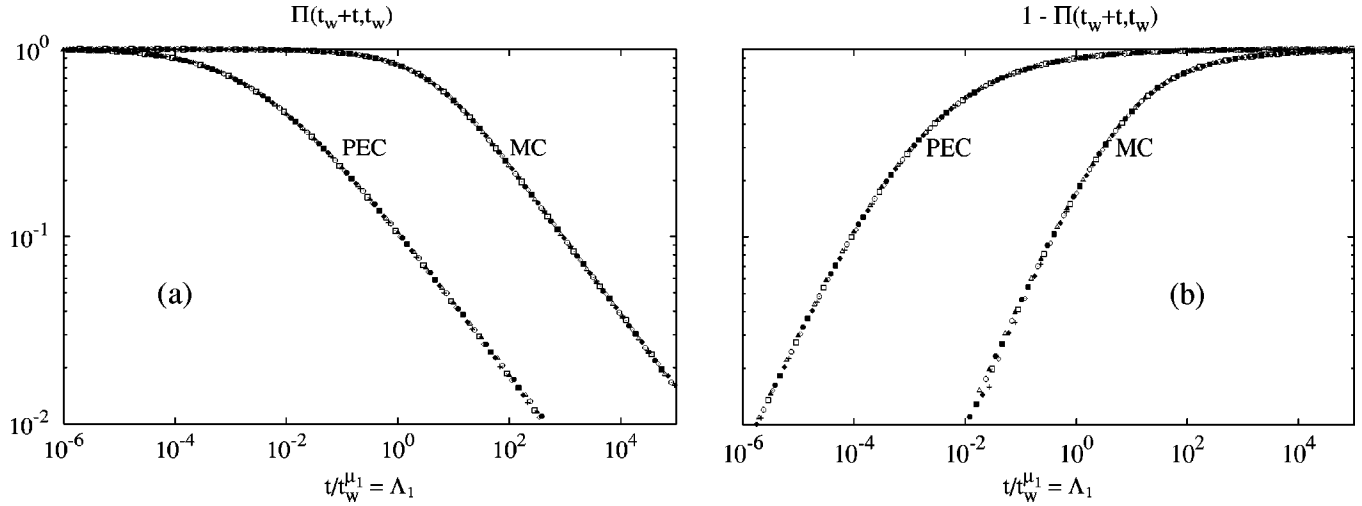

FIG. 8. $\Pi(t_w+t,t_w)$ and $1-\Pi(t_w+t,t_w)$ for $(d,\theta,\alpha)=(10,1/4,3/8)$ as a function of the scaling variable $t/t_w^{\mu_1}$ from Monte Carlo simulations and the partial equilibrium formula, Eq. (13) (PEC). The symbols refer to waiting times $t_w=2\times10^{11}$ (+), 6×10^{11} (◇), 3×10^{12} (♦), 1×10^{13} (□), 4×10^{13} (■), 2×10^{14} (○), 6×10^{14} (●), 3×10^{15} (△), and 1×10^{16} (▲). The tick labels of the ordinate of part (a) refer also to part (b).

$$f(z)=1-\Gamma\left(1-\frac{\theta}{\alpha}\right)z^{\theta/\alpha}-\frac{\theta}{\theta-\alpha}\ z+\mathcal{O}(z^2), \quad (34b)$$

where $\Gamma(a)=\Gamma(a,0)$ is the Gamma function. For $z\to\infty$ $(|\arg z|<3\pi/2)$

$$f(z)\sim\frac{\theta}{\alpha}\frac{e^{-z}}{z}. \quad (34c)$$

In the limit $S\to\infty$ $(t_w\to\infty)$, the asymptotic form of Eq. (32) is [see Eq. (C3)]

$$\tilde{\Pi}(t,S)\sim S\int_0^\infty d\lambda\, e^{-\lambda^\theta\tilde{S}}g(t;\lambda), \quad (35)$$

where

$$\tilde{S}\equiv\kappa S, \quad \kappa\equiv\Gamma(1-\theta). \quad (36)$$

A. First scaling regime: $F_1(\Lambda_1)$

By substituting $u=\tilde{S}^{1/\theta}\lambda$ in Eq. (35) and $v\equiv\tau/\tilde{S}^{1/\theta}$ in Eq. (33) we obtain

$$\tilde{\Pi}(t,S)\sim\frac{\theta}{\kappa}\int_0^\infty du\, e^{-u^\theta}\int_{\tilde{S}^{-1/\theta}}^\infty\frac{dv}{v^\theta}e^{-uv}\int_1^\infty\frac{\theta\, d\tau_1}{\tau_1^{1+\theta}}e^{-u\tau_1/\tilde{S}^{1/\theta}}\times\int_1^\infty\frac{\theta\, d\tau_2}{\tau_2^{1+\theta}}e^{-u\tau_2/\tilde{S}^{1/\theta}}\exp\left(-t\tilde{S}^{-(1-\alpha)/\theta}\frac{\tau_1^\alpha+\tau_2^\alpha}{v^{1-\alpha}}\right)\times\left[f\left(\frac{t\tilde{S}^{-(1-\alpha)/\theta}}{v^{1-\alpha}}\right)\right]^{2(d-1)}. \quad (37)$$

When keeping

$$\Lambda_1\equiv t\tilde{S}^{-(1-\alpha)/\theta} \quad (38)$$

fixed, Eq. (37) has a well-defined limit for $\tilde{S}\to\infty$. Before taking this limit, however, let us note at this point that if we would have considered all τ_{n_j} in Eq. (13) to belong to the Brownian path, we had obtained

$$\tilde{\Pi}(t,S)\sim\frac{\theta}{\kappa}\int_0^\infty du\, e^{-u^\theta}\int_{\tilde{S}^{-1/\theta}}^\infty\frac{dv}{v^\theta}\times e^{-uv}\prod_{i=1}^{2d}\left[\int_1^\infty\frac{\theta\, d\tau_i}{\tau_i^{1+\theta}}\exp\left(-\frac{u\tau_i}{\tilde{S}^{1/\theta}}-\Lambda_1\frac{\tau_i^\alpha}{v^{1-\alpha}}\right)\right] \quad (39)$$

instead of Eq. (37). Now, $v^{-\theta}\exp(-u^\theta-uv)\Pi_{j=1}^{2d}\theta\tau_j^{-1-\theta}$ is an integrable majorant for the integrand in both Eqs. (37) and (39). Hence, by Lebesgue's theorem we obtain from both equations the same scaling function

$$F_1(\Lambda_1)\equiv\frac{\theta}{\kappa}\int_0^\infty du\, e^{-u^\theta}\int_0^\infty\frac{dv}{v^\theta}e^{-uv}\left[f\left(\frac{\Lambda_1}{v^{1-\alpha}}\right)\right]^{2d}. \quad (40)$$

We can conclude that it makes no difference here whether we consider the path of distinct visited sites to have a one dimensional or a compact topology or anything in between. As required by normalization, $F_1(0)=1$.

B. Limit $\Lambda_1\to\infty$

When transforming to variables $\xi\equiv\Lambda_1^{1/(1-\alpha)}u$ and $\zeta\equiv\lambda_1^{-1/(1-\alpha)}v$ in Eq. (40), we find

$$F_1(\Lambda_1)=\Lambda_1^{-\theta/(1-\alpha)}\frac{\theta}{\kappa}\int_0^\infty d\xi\, e^{-\Lambda_1^{-\theta/(1-\alpha)}\xi^\theta}\int_0^\infty d\zeta\,\zeta^{-\theta}\times e^{-\xi\zeta}f^{2d}(\zeta^{-(1-\alpha)}).$$

Since the integrand in the limit $\Lambda_1\to\infty$ is an integrable majorant for all Λ_1, we can take the $\Lambda_1\to\infty$ limit under the integral to obtain

$$F_1(\Lambda_1)\sim c_\infty\Lambda_1^{-\theta/(1-\alpha)} \quad \text{for} \quad \Lambda_1\to\infty, \quad (41a)$$

where

$$c_\infty\equiv\frac{\theta}{\kappa}\int_0^\infty\frac{d\zeta}{\zeta^{1+\theta}}f^{2d}(\zeta^{-(1-\alpha)}). \quad (41b)$$

Note that this integral is well defined because of the asymptotic behavior of $f(.)$ given in Eqs. (34b,c).

C. Limit $\Lambda_1\to 0$

Since $F_1(\Lambda_1)\to 1$ for $\Lambda_1\to 0$, it is convenient to consider

$$1-F_1(\Lambda_1)=\frac{\theta}{\kappa}\int_0^\infty du\, e^{-u^\theta}\int_0^\infty\frac{dv}{v^\theta}e^{-uv}\left[1-f^{2d}\left(\frac{\Lambda_1}{v^{1-\alpha}}\right)\right]. \quad (42)$$

For $\theta<\alpha$ it follows from Eqs. (34a–c) $1-f(x)^{2d}=2d\Gamma(1-\theta/\alpha)x^{\theta/\alpha}\varphi_<(x)$, where $\varphi_<(x)$ is a bounded function, $\varphi_<(x)<M_<$ for $0\leqslant x<\infty$, with $\varphi_<(x)\to 1$ for $x\to 0$. Hence,

$$1-F_1(\Lambda_1)=2d\Gamma\left(1-\frac{\theta}{\alpha}\right)\frac{\theta}{\kappa}\Lambda^{\theta/\alpha}\int_0^\infty du\, e^{-u^\theta}\int_0^\infty\frac{dv}{v^{\theta/\alpha}}\times e^{-uv}\varphi_<\left(\frac{\Lambda_1}{v^{1-\alpha}}\right). \quad (43)$$

Since $M_<v^{-\theta/\alpha}\exp(-uv-u^\theta)$ is an integrable majorant of the integrand, we find

$$1-F_1(\Lambda_1)\sim c_<\Lambda_1^{\theta/\alpha}, \quad \Lambda_1\to 0, \quad \theta<\alpha, \quad (44a)$$

where

$$c_< \equiv \frac{2d\,\theta\Gamma\left(1-\frac{\theta}{\alpha}\right)}{\Gamma(1-\theta)}\int_0^\infty du\, e^{-u^\theta}\int_0^\infty \frac{dv}{v^{\theta/\alpha}}e^{-uv} = \frac{2d\Gamma\left(1-\frac{\theta}{\alpha}\right)^2\Gamma\left(\frac{1}{\alpha}\right)}{\Gamma(1-\theta)}. \quad (44b)$$

For $\theta>\alpha$ the v integral in Eq. (43) would become divergent when taking the $\Lambda_1\to 0$ limit in $\varphi_<(\Lambda_1/v^{(1-\alpha)})$. We thus transform the v variable in Eq. (42), $w\equiv\Lambda_1/v^{1-\alpha}$, to obtain

$$1-F_1(\Lambda_1)=\frac{\theta\Lambda_1^{(1-\theta)/(1-\alpha)}}{(1-\alpha)\kappa}\int_0^\infty du\, e^{-u^\theta}\int_0^\infty \frac{dw}{w^{1+(1-\theta)/(1-\alpha)}} \times[1-f^{2d}(w)]\exp\left(-\frac{u\Lambda_1^{1/(1-\alpha)}}{w^{1/(1-\alpha)}}\right). \quad (45)$$

From Eqs. (34a–c) it follows for $\theta>\alpha$ that $1-f^{2d}(w)=w\varphi_>(w)$, where $\varphi_>(w)$ is a bounded function, $\varphi_>(w)<M_>$ for $0\leqslant w<\infty$, with $\varphi_>(w)\to(\theta-\alpha)/2d\theta$ for $w\to 0$. Hence, $M_>\exp(-u^\theta)w^{(1-\theta)/(1-\alpha)}$ is an integrable majorant of the integrand in Eq. (45) and we can take the $\Lambda_1\to 0$ limit under the integral, yielding

$$1-F_1(\Lambda_1)\sim c_>\Lambda_1^{(1-\theta)/(1-\alpha)},\quad \Lambda_1\to 0,\quad \theta>\alpha, \quad (46a)$$

where

$$c_>=\frac{\Gamma\left(\frac{1}{\theta}\right)}{(1-\alpha)\Gamma(1-\theta)}\int_0^\infty \frac{dw}{w^{1+(1-\theta)/(1-\alpha)}}[1-f^{2d}(w)]. \quad (46b)$$

D. Second scaling regime: $F_2(\Lambda_2)$

The second scaling regime is more difficult to extract from Eqs. (32) and (33). We start by taking advantage of the normalization $\tilde{\Pi}(t=0,S)\sim 1$ in order to write

$$1-\tilde{\Pi}(t,S)\sim\frac{\theta}{\kappa}\int_0^\infty du\, e^{-u^\theta}\int_{\tilde{S}^{-1/\theta}}^\infty \frac{dv}{v^\theta}e^{-uv}\left(\prod_{j=1}^{2d}\int_1^\infty\frac{\theta\, d\tau_j}{\tau_j^{1+\theta}}\right) \times\exp\left(-\frac{u}{\tilde{S}^{1/\theta}}\sum_{k=1}^n\tau_k\right) \times\left[1-\exp\left(-\frac{\Lambda_1}{v^{1-\alpha}}\sum_{j=1}^{2d}\tau_j^\alpha\right)\right]. \quad (47)$$

This corresponds to Eqs. (37) and (39), if the number of neighboring sites belonging to the Brownian path is n, $2\leqslant n\leqslant 2d$ (see the discussion in Sec. IV).

After the transformation $v\to w=\Lambda_1\Sigma_{j=1}^{2d}\tau_j^\alpha/v^{(1-\alpha)}$ this can be rewritten as

$$1-\tilde{\Pi}(t,S)\sim\frac{\theta\Lambda_1}{(1-\alpha)\kappa}\int_0^\infty du\, e^{-u^\theta}u^{-(\alpha-\theta)}\left(\prod_{j=1}^{2d}\int_1^\infty\frac{\theta\, d\tau_j}{\tau_j^{1+\theta}}\right) \times\exp\left(-\frac{u}{\tilde{S}^{1/\theta}}\sum_{k=1}^n\tau_k\right)\left(\sum_{j=1}^{2d}\tau_j^\alpha\right) \times\left[\Lambda_1 u^{1-\alpha}\sum_{j=1}^{2d}\tau_j^\alpha\right]^{(1-\theta)/(1-\alpha)-1} \times\int_0^{t\Sigma_{j=1}^{2d}\tau_j^\alpha}\frac{dw(1-e^{-w})}{w^{1+(1-\theta)/(1-\alpha)}} \times\exp\left[-\left(\frac{\Lambda_1 u^{1-\alpha}\sum_{j=1}^{2d}\tau_j^\alpha}{w}\right)^{1/(1-\alpha)}\right].$$

We now decompose this expression into the sum of two parts corresponding to a decomposition $\Sigma_{j=1}^{2d}\tau_j^\alpha=\Sigma_{j=1}^{n}\tau_j^\alpha+\Sigma_{j=n+1}^{2d}\tau_j^\alpha$ in the second line. We can use the symmetry with respect to $\{\tau_j\}$ in order to replace $\Sigma_{j=1}^n\tau_j^\alpha$ by $n\tau_1^\alpha$ in the first part and $\Sigma_{j=n+1}^{2d}\tau_j^\alpha$ by $(2d-n)\tau_{2d}^\alpha$ in the second part. After the transformation $\zeta=\tilde{S}^{-1/\theta}\tau_1$ in the first part, and the transformation $\zeta=\tilde{S}^{-1/\theta}\tau_{2d}$ in the second part one can, for $\theta<\alpha$, again use Lebesgue's theorem to perform the limit $S\to\infty$ for fixed

$$\Lambda_2\equiv\tilde{S}^{\alpha/\theta}\Lambda_1=\frac{t}{\tilde{S}^{(1-2\alpha)/\theta}},\quad \theta<\alpha<\frac{1}{2}. \quad (48)$$

This yields

$$\tilde{S}[1-\Pi(t,S)]\sim F_2(\Lambda_2) \quad (49a)$$

$$F_2(\Lambda_2)=nF_2^{(1)}(\Lambda_2)+(2d-n)F_2^{(2)}(\Lambda_2), \quad (49b)$$

where

$$F_2^{(1)}(\Lambda_2)\equiv\frac{\theta^2\Lambda_2}{(1-\alpha)\kappa}\int_0^\infty\frac{du\, e^{-u^\theta}}{u^{\alpha-\theta}}\int_0^\infty\frac{d\zeta e^{-u\zeta}}{\zeta^{1-(\alpha-\theta)}}h(\Lambda_2 u^{1-\alpha}\zeta^\alpha), \quad (50)$$

$$h(x)\equiv x^{(1-\theta)/(1-\alpha)-1}\int_0^\infty\frac{dw(1-e^{-w})}{w^{1+1-\theta/1-\alpha}}\exp[-(x/w)^{1/(1-\alpha)}], \quad (51)$$

and

$$F_2^{(2)}(\Lambda_2)\equiv\frac{\theta^2\Lambda_2}{(1-\alpha)\kappa}\int_0^\infty\frac{du\, e^{-u^\theta}}{u^{\alpha-\theta}}\int_0^\infty\frac{d\zeta h(\Lambda_2 u^{1-\alpha}\zeta^\alpha)}{\zeta^{1-(\alpha-\theta)}} =\frac{\theta^2\Lambda_2^{\theta/\alpha}}{\alpha(1-\alpha)\kappa}\int_0^\infty\frac{du\, e^{-u^\theta}}{u^{1-\theta/\alpha}}\int_0^\infty\frac{dv\, h(v)}{v^{\theta/\alpha}} =\frac{\Gamma\left(1-\frac{\theta}{\alpha}\right)^2\Gamma\left(\frac{1}{\alpha}\right)}{\Gamma(1-\theta)}\Lambda_2^{\theta/\alpha}. \quad (52)$$

The restriction to $\alpha<1/2$ in Eq. (48) follows from the fact that in order for the scaling regime to be relevant, $t_2 \sim \tilde{S}^{(1-2\alpha)/\theta} \sim t_w^{\gamma(1-2\alpha)/\theta}$ should increase with increasing t_w. The function $h(x)$ has the asymptotic behavior

$$h(x) \sim \begin{cases} (1-\alpha)\Gamma(\alpha-\theta), & x \to 0^+ \\ (1-\alpha)\Gamma(1-\theta)x^{-1}, & x \to \infty. \end{cases} \tag{53}$$

The importance of the condition $\theta<\alpha$ now becomes clear, since for the ζ integrand to be integrable in Eqs. (50) and (52) for $\zeta \to 0$, $\alpha-\theta$ has to be positive.

E. Limit $\Lambda_2 \to \infty$

After the transformation $\zeta \to v = \Lambda_2 u^{(1-\alpha)} \zeta^\alpha$, Eq. (50) gives

$$F_2^{(1)}(\Lambda_2) = \frac{\theta^2 \Lambda_2^{\theta/\alpha}}{\alpha(1-\alpha)\kappa} \int_0^\infty \frac{du}{u^{1-\theta/\alpha}} e^{-u^\theta} \int_0^\infty \frac{dv}{v^{\theta/\alpha}} \times \exp[-uv^{1/\alpha}\Lambda_2^{-1/\alpha} u^{-(1-\alpha)/\alpha}] h(v). \tag{54}$$

The limit $\Lambda_2 \to \infty$ can then be taken under the integral, yielding [cf. Eq. (52)]

$$F_2^{(1)}(\Lambda_2) \sim F_2^{(2)}(\Lambda_2). \tag{55}$$

Using Eqs. (49b) and (52) we finally obtain

$$F_2(\Lambda_2) \sim c_2^{(\infty)} \Lambda_2^{\theta/\alpha}, \quad c_2^{(\infty)} \equiv \frac{2d\Gamma\left(1-\frac{\theta}{\alpha}\right)^2 \Gamma\left(\frac{1}{\alpha}\right)}{\Gamma(1-\theta)}. \tag{56}$$

As required by matching, $c_2^{(\infty)} = c_<$ [cf. Eq. (44b)].

F. Limit $\Lambda_2 \to 0$

Since $h(x)$ is monotonously decreasing with x for $x>0$, we can replace $h(\Lambda_2 u^{1-\alpha}\zeta^\alpha)$ by $h(0) = (1-\alpha)\Gamma(\alpha-\theta)$ in Eq. (50). Hence,

$$F_2^{(1)}(\Lambda_2) \sim c_2 \Lambda_2, \tag{57}$$

where

$$c_2 \equiv \frac{\theta^2 \Gamma(\alpha-\theta)}{\kappa} \int_0^\infty \frac{du\, e^{-u^\theta}}{u^{\alpha-\theta}} \int_0^\infty \frac{d\zeta\, e^{-u\zeta}}{\zeta^{1-(\alpha-\theta)}} = \frac{\theta}{1-\alpha} \frac{\Gamma(\alpha-\theta)\Gamma\left(\frac{1-2(\alpha-\theta)}{\theta}\right)}{\Gamma(1-\theta)}. \tag{58}$$

This means that for small Λ_2, $F_2(\Lambda_2)$ should be dominated by $F_2^{(2)}(\Lambda_2)$, except for $d>1$ [where $F_2(\Lambda_2) = 2F_2^{(1)}(\Lambda_2)$]. For a given (mean) value of n we thus find

$$F_2(\Lambda_2) \sim c_2^{(0)} \Lambda_2^{\theta/\alpha}, \quad c_2^{(0)} \equiv \left(1-\frac{n}{2d}\right) c_2^{(\infty)}. \tag{59}$$

This $\Lambda_2 \to 0$ limit of the generalized scaling form depends on the number of neighbors being considered to belong to the Brownian path (see the discussion in Sec. IV). According to Eq. (57), there can occur an intermediate regime, where $F_2(\Lambda_2)$ depends linearly on Λ_2. This intermediate regime seems to be more pronounced for the "true dynamics" (see Fig. 7) than for the dynamics predicted by the PEC formula (13).

VIII. SUMMARY AND CONCLUSIONS

We have studied aging within the framework of a simple hopping model mimicking a system that performs thermally activated transitions between the deep free-energy minima of its configuration space. Based on general arguments from the statistical theory of extremes we have chosen the free-energy density of states to exhibit an exponential tail. In order to effectively quantify the influence of the initial and target site on the energy barrier to be surmounted during a transition, we introduced a parameter α, $0 \leqslant \alpha < 1$, in the hopping rates that turned out to strongly influence the aging properties. We have found that generically, subaging occurs in these models, an effect related to the multiple visits of deep traps. We have also found that different time scales, corresponding to different scaling regions, appear in these models.

These aging properties can be understood from a PEC that, despite not being an exact quantitative description, provides a powerful tool to study the scaling properties of the aging dynamics. Based on the PEC we first motivated the occurrence of subaging behavior and generalized scaling forms in terms of simple scaling arguments. We then presented a detailed analysis of the PEC formula (13) and calculated the aging functions following from Eq. (13) and their asymptotics exactly. With respect to the scaling properties the predictions could be confirmed by Monte Carlo simulations in $d=1$, 10, 100, and 1000 dimensions.

The fact that even for $d=1000$ the "quenched model" has aging properties different from the "annealed model" studied earlier in Ref. 35 is rather surprising, since the number of distinct visited sites S in $d>2$ scales as the number of all transitions N between minima for large N, $S \sim N$. From this one tends to conclude that the system effectively explores a new minimum in each transition, which would correspond to the annealed situation. However, in the quenched situation one can imagine that there is always some *local* equilibrium established at the site with minimal energy reached after time t_w, and this local equilibration effect slows down the diffusion in configuration space on all time scales, i.e. instead of $S \sim N \sim t_w^{\theta'}$ with $\theta' = \min[1, \theta/(1-\alpha)]$ in the annealed situation we have $S \sim N \sim t_w^\theta$ in the quenched situation for $d>2$, $0<\theta<1$.

The existence of a local equilibrium around the "dominant" site with minimal energy after time t_w does not imply that there must be a true equilibration on all visited sites as it is assumed in the PEC formula (13). In fact, by studying the disorder averaged participation ratios $Y_q(t) \equiv \langle \Sigma_j P_j(t)^q \rangle$, where $P_j(t)$ is the probability for the system to be at minimum j at time t, we find that the PEC never becomes exact in the limit $t \to \infty$, not even in $d=1$ where each trap is visited an infinite number of times. This behavior offers the possibility to define an effective temperature in the nonequilib-

rium aging regime, which enters a modified fluctuation-dissipation theorem, similar as it was found for mean-field spin-glass models.[38] The role of an effective temperature in the landscape model considered here will be discussed elsewhere[46] (for recent progress in our understanding of this problem coming from MD simulations, see Ref. 47).

With respect to the applicability of the analysis outlined above the question arises, whether the characteristics of the aging dynamics can be worked out also for general hopping rates not exhibiting the specific form given in Eq. (3). For the PEC to be applicable, the system should have the tendency to approach equilibrium (that truly exists only for $\theta>1$), so that one may require the jump rates to obey detailed balance. It is then indeed straightforward, by using the simple arguments presented in Sec. V, to extract all characteristic time scales $t_j(t_w)$ and to predict the scaling properties. A necessary ingredient for this procedure to work correctly, however, is the robustness of the scaling relation $S(t_w)\sim t_w^{\gamma}$ [cf. Eqs. (14a,b)]. Preliminary results indicate that for ''physical choices'' of the jump rates (meaning that the dependence of the energies of the initial and target site on the saddle point energy is reasonable), Eqs. (14a,b) always hold true.

Moreover, it is possible also to consider some random distribution of the form of the jump rates (as it is expected to occur when the dynamics in configuration space is mapped onto a jump process by means of some quantitative analysis), and to work out the aging features of such more realistic models. It turns out then, that in principle infinitely many aging regimes can exists in the two-time plane $t,t_w\geqslant 0$. A thorough discussion of these issues, however, is beyond the scope of the present work.

ACKNOWLEDGMENTS

We should like to thank W. Dieterich and E. Bertin for stimulating discussions. P.M. gratefully acknowledges financial support from the Deutsche Forschungsgemeinschaft through the Heisenberg program (Ma 1636/2-1).

APPENDIX A: TECHNICAL DETAILS OF THE MONTE CARLO SIMULATIONS

We use the standard continuous-time Monte Carlo algorithm as discussed in detail, e.g., in Ref. 48 to simulate the stochastic process defined in Sec. II A. A special problem arises for large dimensions $d\gg 1$, where it is not possible to save the energies within a hypercube of even small linear dimension. To resolve this problem, we use hash maps, as, for example, the hash map template provided by the Standard Template Library of ISO–C++.

The hash function should be computable quickly and at the same time the sites **x** being encountered must be mapped to different hash values as often as possible. For dimensions $d\geqslant 10$ we found

$$f(\mathbf{x})=\sum_{n=1}^{2d} n x_n \tag{A1}$$

to do a good job. For large d the RAM consumption of the computer programs is the limiting factor when trying to access longer times t_w. While simulations for $d\leqslant 10$ can easily be performed on workstations, for $d\geqslant 100$ computers with 4GB of RAM and more are necessary.

APPENDIX B: CONNECTION BETWEEN THE "NUMBER OF DISTINCT VISITED SITES" AND THE WAITING TIME

For $\alpha=0$, i.e. the trap model, we use a scaling argument discussed in Ref. 49 to derive the behavior of $S(t_w)$ for large t_w. Then we show by a finite-size scaling argument that in $d=1$ the behavior of $S(t_w)$ for $\alpha=0$ is not expected to change for $0<\alpha<1$. Furthermore, we give general arguments for the invariance of Eq. (14b) with respect to α for all d. Finally we confirm Eqs. (14a,b) by Monte Carlo simulations.

1. Trap model ($\alpha=0$)

After $N\gg 1$ transitions of the system, the typical elapsed time t_w is

$$\begin{aligned} t_w(N)\simeq\sum_{i=1}^{N}\tau_i &\simeq N\sum_{\mu}\frac{g_\mu(N)}{N}\tau_\mu\Delta\tau_\mu \\ &\sim N\int_1^{\tau_{\max}(S(N))} d\tau\,\tau\rho(\tau) \\ &\sim N[\tau_{\max}(S(N))]^{(1-\theta)}, \end{aligned} \tag{B1}$$

where $g_\mu(N)$ is the typical number of τ_j falling in some interval $\tau_\mu-\Delta\tau_\mu/2\leqslant\tau_\mu\leqslant\tau_\mu+\Delta\tau_\mu/2$, $S(N)$ is the typical number of distinct visited sites after N jumps and $\tau_{\max}(S)$ is the typical maximal τ obtained after the system encountered S distinct sites.

Since $\tau_{\max}(S)\sim S^{1/\theta}$ and (see, e.g., Ref. 50)

$$S(N)\sim\begin{cases} N^{d/2}, & 1\leqslant d<2 \\ N/\ln N, & d=2 \\ N & d>2, \end{cases} \tag{B2}$$

we find

$$t_w(S)\sim\begin{cases} S^{[d+(2-d)\theta]/d\theta}, & 1\leqslant d<2 \\ S^{1/\theta}\ln S & d=2 \\ S^{1/\theta}, & d>2. \end{cases} \tag{B3}$$

This yields Eqs. (14a,b) for $\alpha=0$.

We note that in the annealed model Eq. (B2) remains valid, while $\tau_{\max}\sim N^{1/\theta}$, leading to $S(t_w)\sim t_w^{d\theta/2}$ for $1\leqslant d<2$, $S(t_w)\sim t_w^{\theta}/\ln t_w$ for $d=2$, and $S(t_w)\sim t_w^{\theta}$ for $d>2$. Due to our discussion in Sec. III, one can replace θ by $\theta'=\min[1,\theta/(1-\alpha)]$ in these formulas to obtain the behavior for $0\leqslant\alpha<1$.

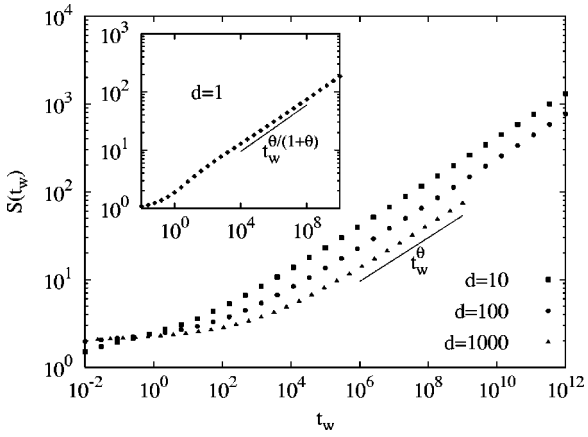

FIG. 9. Number of distinct visited sites $S(t_w)$ for $(\theta,\alpha)=(1/4,3/8)$ and different dimensions d.

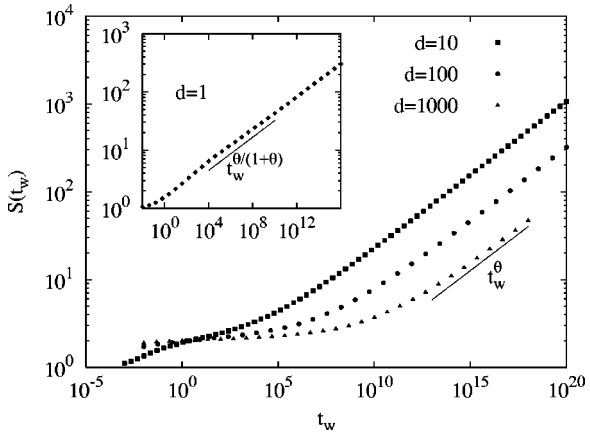

FIG. 10. Number of distinct visited sites $S(t_w)$ for $(\theta,\alpha)=(1/6,1/4)$ and different dimensions d.

2. One dimension ($0\leqslant\alpha<1$)

Let us consider a finite chain with L sites and site energies distributed according to Eq. (1). Then the mean-square displacement $\langle\Delta x^2(t)\rangle$ of a particle performing a random walk on this chain with the hopping rates given in Eq. (3) is expected to scale as

$$\langle\Delta x^2(t)\rangle\sim\begin{cases} t^{\eta} & \text{for} \quad \langle\Delta x^2(t)\rangle\ll L^2 \\ D(L)t & \text{for} \quad \langle\Delta x^2(t)\rangle\gg L^2 \end{cases} \tag{B4}$$

for large L. The diffusion coefficient $D(L)$ can be written as[51]

$$D(L)=\frac{L^2}{\sum_{j=1}^{L}\left(p_j^{(\mathrm{eq})}w_{j,j+1}\right)^{-1}} \tag{B5}$$

with $p_j^{(\mathrm{eq})}=\exp(-\beta E_j)/\Sigma_{k=1}^{L}\exp(-\beta E_k)=\tau_j/\Sigma_k\tau_k$. The denominator then reads, using Eq. (8), $\Sigma_{i=1}^{L}\tau_i\Sigma_{j=1}^{L}(\tau_j\tau_{j+1})^{-\alpha}$. Since $\langle(\tau_j\tau_{j+1})^{-\alpha}\rangle$ exists (for $\alpha>-\theta$), the second sum gives a contribution $\propto L$ for large L, while the first sum has no finite average and is dominated by the maximum $\tau_{\max}\sim L^{1/\theta}$. Thus we find

$$D(L)\sim\frac{L^2}{L^{1/\theta}L}\sim L^{1-1/\theta}. \tag{B6}$$

At the crossover time t_x, where $\langle\Delta x^2(t_x)\rangle$ changes its behavior in Eq. (B4), we obtain from continuity

$$t_x^{\eta}\sim D(L)t_x\sim L^2. \tag{B7}$$

This implies $t_x\sim L^{2/\eta}$ and $t_x\sim L^{1+1/\theta}$ yielding

$$\eta=\frac{2\theta}{1+\theta}. \tag{B8}$$

Since $S(t_w)\sim\langle\Delta x^2(t)\rangle^{1/2}$, we finally obtain for $0\leqslant\alpha<1$

$$S(t_w)\sim t_w^{\eta/2}=t_w^{\theta/(1+\theta)} \tag{B9}$$

in agreement with Eqs. (14a,b).

3. General arguments

The very physical difference between the trap model ($\alpha=0$) and models with weighted rates ($\alpha>0$) is the occurrence of forward-backward jump correlations. When the system jumps from a site with low-energy to a site with energy close to zero (such energies are most likely), it has high tendency to jump back for $\alpha>0$. More generally, when the system enters a region of connected low-energy sites, it will, before escaping this region, perform more and more jumps between the low energy sites the larger the value of α is. Once it leaves the region, it again has high tendency to jump back to it.

One may regard a cluster of sites with deep energies and the surrounding shell of sites with higher energy as a ''supertrap.'' On a coarse-grained level with respect to time, the particle performs ''superhops'' between these supertraps. Then the essential difference between the $\alpha=0$ and the $\alpha>0$ situation disappears, since there are no increased backward jump correlations between the superhops. One thus suspects that α only rescales the time t_w of the $S(t_w)$ relation but does not change its exponent. Indeed this is what we have shown more explicitly in $d=1$ in the previous section, and there is no reason why the argument should fail in higher dimensions.

It is worth noting that the same arguments also apply to $\Pi(t+t_w,t_w)$, if one generalizes it to a quantity $\Pi_n(t+t_w,t_w)$ that is defined as the averaged probability that the system after a waiting time t_w does not leave a region of radius n in configuration space. Clearly, $\Pi(t+t_w,t_w)=\Pi_0(t+t_w,t_w)$, but for larger n only superhops should lead to a decrease in $\Pi_n(t+t_w,t_w)$. In fact we found that for $n\geqslant 1$ $\Pi_n(t+t_w,t_w)$ shows normal aging, i.e., $\Pi_n(t+t_w,t_w)\sim F_1^{(n)}(t/t_w)$ for $\alpha>0$.

4. Monte Carlo results

Figures 9 and 10 show $S(t_w)$ from Monte Carlo simulations in $d=1$, 10, 100, and 1000 for parameter sets $(\theta,\alpha)=(1/4,3/8)$ and $(1/6,1/4)$, respectively. In all cases $S(t_w)$ shows the behavior predicted by Eqs. (14a,b).

APPENDIX C: $\tilde{\Pi}(T,S)$ IN THE LIMIT $S\to\infty$

To derive the large S limit of Eq. (32),

$$\tilde{\Pi}(t,S)=S\int_0^\infty d\lambda\langle e^{-\lambda\tau}\rangle^{S-3}g(t;\lambda), \tag{C1}$$

we need to consider the small λ limit of

$$\langle e^{-\lambda\tau}\rangle=\int_1^\infty\frac{\theta d\tau}{\tau^{1+\theta}}e^{-\lambda\tau}=\theta\lambda^\theta\Gamma(-\theta,\lambda)$$

$$=1-\Gamma(1-\theta)\lambda^\theta+\frac{\theta}{1-\theta}\lambda+\mathcal{O}(\lambda^2)$$

$$\equiv e^{-\varphi(\lambda)\lambda^\theta},$$

where $\varphi(\lambda)$ is a continuous function with $\varphi(\lambda)\to\Gamma(1-\theta)$ for $\lambda\to0$. Furthermore, $\langle e^{-\lambda\tau}\rangle$ has an upper bound $e^{-a\lambda^\theta}$ for $\lambda\geqslant0$,

$$\langle e^{-\lambda\tau}\rangle<e^{-a\lambda^\theta} \tag{C2}$$

with some constant a, $0<a\leqslant1$, being independent of λ. To prove this for $\lambda\geqslant1$ we compare

$$e^{-a\lambda^\theta}=\int_1^\infty d\tau[a\lambda^\theta\tau^{-1+\theta}e^{-a(\lambda\tau)^\theta}]$$

with

$$\langle e^{-\lambda\tau}\rangle=\int_1^\infty d\tau[\theta\tau^{-1-\theta}e^{-\lambda\tau}].$$

For $\theta\leqslant a\leqslant1$ and $\tau\geqslant1$ the first integrand is larger than the second integrand for all $\lambda\geqslant1$, thus the first integral is larger than the second integral. Since $e^{-a\lambda^\theta}$ for fixed λ is strictly monotonously decreasing with a this remains valid also for $0<a<\theta$. To prove property (C2) for $\lambda<1$ we note that for small argument ϵ it is

$$e^{-\varphi(\epsilon)\epsilon^\theta}+\mathcal{O}(\epsilon)=1-\Gamma(1-\theta)\epsilon^\theta$$

$$<1-a\epsilon^\theta=e^{-a\epsilon^\theta}+\mathcal{O}(\epsilon^{2\theta}),$$

since $\Gamma(1-\theta)>1$ for $\theta<1$. We can deduce that it exists a finite interval $(0,\lambda_0]$ where Eq. (C2) holds. Because $\langle e^{-\lambda\tau}\rangle$ is strictly monotonously decreasing it is $\langle e^{-\lambda_0\tau}\rangle<1$. When choosing $a_0\equiv-\ln\langle e^{-\lambda_0\tau}\rangle>0$ it holds that

$$\langle e^{-\lambda\tau}\rangle<e^{-a_0\lambda^\theta}\ \text{ for }\ 0<\lambda\leqslant1$$

and the proof of Eq. (C2) is complete.

With the transformation $\lambda\to u\equiv S^{1/\theta}\lambda$ Eq. (C1) gives

$$\tilde{\Pi}(t,S)=\int_0^\infty du\,\exp\left(-\varphi(u^\theta/S)\frac{S-3}{S}u^\theta\right)S^{1-1/\theta}g\left(t;\frac{u}{S^{1/\theta}}\right).$$

When using Eq. (C2) we can estimate

$$\exp\left[-\varphi(u^\theta/S)\frac{S-3}{S}u^\theta\right]<\exp\left(-a\frac{S-3}{S}u^\theta\right)<\exp\left(-\frac{a}{2}u^\theta\right)$$

for $S>6$ and from Eq. (33),

$$S^{1-1/\theta}g(t;S^{-1/\theta}u)\leqslant S^{1-1/\theta}\int_1^\infty\frac{\theta d\tau}{\tau^\theta}e^{-S^{-1/\theta}u\tau}$$

$$=S^{1-1/\theta}\theta\lambda^{\theta-1}\Gamma(1-\theta,S^{-1/\theta}u)$$

$$\leqslant\theta\Gamma(1-\theta)u^{\theta-1}.$$

These estimations will allow us to use Lebesgue's theorem when considering the limit $S\to\infty$ in Eqs. (37) and (47). Thus we can write asymptotically

$$\tilde{\Pi}(t,S)\sim S^{1-1/\theta}\int_0^\infty du\,e^{-\kappa u^\theta}g(t;S^{-1/\theta}u)$$

$$\sim S\int_0^\infty d\lambda\,e^{-\lambda^\theta\kappa S}g(t;\lambda), \tag{C3}$$

where the shortcut $\kappa=\Gamma(1-\theta)$ [cf. Eq. (36)] has been used.

[1] *Glasses and Amorphous Materials*, edited by J. Zarzycki, Materials Science and Technology, Vol. 9 (VCH, Weinheim, 1991).

[2] G. Parisi, cond-mat/9910375 (unpublished).

[3] L. C. E. Struick, *Physical Aging in Amorphous Polymers and Other Materials* (Elsevier, Houston, 1978).

[4] E. Vincent, J. Hammann, M. Ocio, J. P. Bouchaud, and L. Cugliandolo, in *Complex Behaviour of Glassy Systems*, edited by M. Rubi, Lecture Notes in Physics Vol. 492 (Springer-Verlag, Berlin, 1997), pp. 184–219, and references therein.

[5] P. Nordblad, in *Spin Glasses and Random Fields*, edited by P. Young (World Scientific, Singapore, 1998).

[6] F. Alberici, P. Doussineau, and A. Levelut, J. Phys. I **7**, 329 (1997); F. Alberici, P. Doussineau, and A. Levelut, Europhys. Lett. **39**, 329 (1997).

[7] J. P. Bouchaud, P. Doussineau, T. de Lacerda-Aroso, and A. Levelut, cond-mat/0011190 (unpublished), and references therein.

[8] R. L. Leheny and S. R. Nagel, Phys. Rev. B **57**, 5154 (1998).

[9] L. Bellon, S. Ciliberto, and C. Laroche, Europhys. Lett. **51**, 551 (2000).

[10] W. Kob and J. L. Barrat, Eur. Phys. J. B **13**, 319 (2000).

[11] L. Cipelliti, S. Mansley, R. C. Ball, and D. A. Weitz, Phys. Rev. Lett. **84**, 2275 (2000).

[12] C. Derec, A. Ajdari, G. Ducouret, and F. Lequeux, C. R. Acad. Sci. **1**, 1115 (2000).

[13] M. Cloitre, R. Borrega, and L. Leibler (unpublished).

[14] A. Knaebel, M. Bellour, J.-P. Munch, V. Viasnoff, F. Lequeux, and J. L. Harden, Europhys. Lett. **52**, 73 (2000).

[15] B. Abou, D. Bonn, and J. Meunier, cond-mat/0101327 (unpublished).

[16] L. Bellon, S. Ciliberto, and C. Laroche, Europhys. Lett. **53**, 511 (2001).

[17] A. Vaknin, Z. Ovadyahu, and M. Pollak, Phys. Rev. Lett. **5**, 3402 (2001).

[18] E. Vincent, V. Dupuis, M. Alba, J. Hammann, and J. P. Bouchaud, Europhys. Lett. **50**, 674 (2000).
[19] M. Nicodemi and H. J. Jensen, cond-mat/0103070 (unpublished).
[20] E. Pitard and E. Shaknovitch, cond-mat/9910431 (unpublished).
[21] A. Barrat and V. Loreto, Europhys. Lett. **53**, 297 (2001).
[22] D. Head, Phys. Rev. E **62**, 2439 (2000).
[23] J. P. Bouchaud, L. Cugliandolo, J. Kurchan, and M. Mézard, in *Spin-glasses and Random Fields*, edited by A. P. Young (World Scientific, Singapore, 1998), and references therein.
[24] A. J. Bray, Adv. Phys. **43**, 357 (1994).
[25] J. Kurchan and L. Laloux, J. Phys. A **29**, 1929 (1996).
[26] A. Cavagna, Europhys. Lett. **53**, 490 (2001).
[27] C. Donati, F. Sciortino, and P. Tartaglia, Phys. Rev. Lett. **85**, 1464 (2000).
[28] L. Angelani, R. Di Leonardo, G. Ruocco, A. Scala, and F. Sciortino, Phys. Rev. Lett. **85**, 5356 (2000).
[29] K. Broderix, K. K. Bhattacharya, A. Cavagna, A. Zippelius, and I. Giardina, Phys. Rev. Lett. **85**, 5360 (2000).
[30] M. Goldstein, J. Chem. Phys. **51**, 3728 (1969).
[31] C. A. Angell, Science **267**, 1924 (1995).
[32] J. P. Bouchaud, J. Phys. I **2**, 1705 (1992).
[33] M. Feigel'man and V. Vinokur, J. Phys. (France) **49**, 1731 (1988).
[34] J. P. Bouchaud and D. S. Dean, J. Phys. I **5**, 265 (1995).
[35] C. Monthus and J. P. Bouchaud, J. Phys. A **29**, 3847 (1996).
[36] P. Sollich, F. Lequeux, P. Hebraud, and M. Cates, Phys. Rev. Lett. **70**, 2020 (1997); P. Sollich, Phys. Rev. E **58**, 738 (1998); S. Fielding, P. Sollich, and M. Cates, cond-mat/9907101 (unpublished).
[37] D. S. Fisher, P. Le Doussal, and C. Monthus, Phys. Rev. E **59**, 4795 (1999).
[38] L. Cugliandolo and J. Kurchan, J. Phys. A **27**, 5749 (1994).
[39] L. Berthier, J.-L. Barrat, and J. Kurchan, Phys. Rev. E **63**, 016105 (2001).
[40] B. Rinn, P. Maass, and J. P. Bouchaud, Phys. Rev. Lett. **84**, 5403 (2000).
[41] P. Embrechts, C. Klüppelberg, and Th. Mikosch, *Modelling Extremal Events* (Springer, Berlin, 1997).
[42] J. P. Bouchaud and M. Mézard, J. Phys. A **30**, 7997 (1997).
[43] J. C. Schön and P. Sibani, Europhys. Lett. **49**, 196 (2000).
[44] B. Derrida, Phys. Rev. B **24**, 2613 (1981).
[45] J. P. Bouchaud, in *Soft and Fragile Matter*, edited by M. E. Cates and M. Evans (Institute of Physics, London, 2000).
[46] E. Bertin, J. P. Bouchaud, and P. Maass (unpublished).
[47] F. Sciortino and P. Tartaglia, Phys. Rev. Lett. **86**, 107 (2001).
[48] K. Binder and D. W. Heermann, *Monte Carlo Simulations in Statistical Physics*, Springer Series in Solid State Science, Vol. 80, 2nd ed. (Springer, Berlin, 1992).
[49] H. Harder, S. Havlin, and A. Bunde, Phys. Rev. B **36**, 3874 (1987).
[50] B. D. Hughes, *Random Walks in Random Environments* (Clarendon Press, Oxford, 1995), Vol. I.
[51] R. Kutner, D. Knödler, P. Pendzig, R. Przenioslo, and W. Dieterich, in *Diffusion Processes: Experiment, Theory, Simulations*, edited by A. Pekalski, Lecture Notes in Physics Vol. 438 (Springer-Verlag, Heidelberg, 1994), p. 197.